

Extending Self-Similarity for Fractional Brownian Motion

Lance M. Kaplan and C.-C. Jay Kuo

Abstract—The fractional Brownian motion (fBm) model has proven to be valuable in modeling many natural processes because of its persistence for large time lags. However, the model is characterized by one single parameter that cannot distinguish between short- and long-term correlation effects. This work investigates the idea of extending self-similarity to create a correlation model that generalizes discrete fBm referred to as asymptotic fBm (afBm). Namely, afBm is parameterized by variables controlling short- and long-term correlation effects. We propose a fast parameter estimation algorithm for afBm based on the Haar transform, and we demonstrate the performance of this parameter estimation algorithm with numerical simulations.

I. INTRODUCTION

Many natural processes such as the cross-section of a mountain range, weather data, electrical measurements, and even man-made phenomena such as economic and traffic flow data have been observed to have significant correlation for large time lags [9], [13]. In fact, no exponentially decaying correlation model (e.g., finite-order ARMA models) can capture the long-term correlation structure of such processes. Fractal correlation models such as fractional Brownian motion (fBm) [11], discrete fractional Gaussian noise (dfGn) [11], and fractionally differenced Gaussian noise (fdGn) [4], [6] have been applied as correlation models for many natural processes. These models are characterized by a hyperbolic correlation decay as time lag grows, and the rate of hyperbolic decay is controlled by a single number known as the Hurst parameter. In other words, the Hurst parameter determines the persistence of the correlation as the time lag increases.

Although fractal models have proven useful to distinguish the differences between many natural processes, these models are limited in the sense that the correlation for small time lags is completely determined by the Hurst parameter. As a result, the fractal model cannot find the differences between two processes that have the same persistence but different correlation for time lags near zero. In an effort to design stationary correlation models that handle both short- and long-term correlations, Hosking proposed to consider filtered fractals such that fdGn is passed through a rational (i.e., ARMA) filter [6]. Deriche and Tewfik have implemented a maximum likelihood technique to estimate the parameters of the fdGn process and the ARMA filter [2]. The algorithm is, however, computationally intensive.

The shortcomings motivate us to generalize the fractal models by a different approach. We consider extending the idea of self-similarity that characterizes fBm and dfGn such that the variance of the increments of a process is related to a certain function of scale, i.e., the structure function, and we call the resulting processes the extended self-similar (ESS) processes. Because one can create a structure function parameterized to measure different correlation effects, the new ESS concepts should be useful for synthesis, classification, and segmentation of signals, textures, or landscapes. To show the

Manuscript received September 19, 1993; revised May 16, 1994. This work was supported by a National Science Foundation Graduate Fellowship and the National Science Foundation Presidential Faculty Fellow (PFF) Award ASC-9350309. The associate editor coordinating the review of this paper and approving it for publication was Dr. Thomas F. Quatieri.

The authors are with the Signal and Image Processing Institute and the Department of Electrical Engineering-Systems, University of Southern California, Los Angeles, CA 90089-2564 USA.

IEEE Log Number 9406033.

application of ESS processes, we consider an ESS-based model we refer to as *asymptotic fBm* that has one parameter to control the short-term correlation and another parameter to control the persistence of a random signal. Fast Hurst parameter estimation algorithms for fBm processes based on the wavelet transform [7], [15] motivate us to use a wavelet transform for a fast parameter estimation of the asymptotic fBm model.

This correspondence is organized as follows. The theoretical properties of ESS processes appear in Section II. Section III introduces asymptotic fBm and a parameter estimation algorithm. Finally, Section IV concludes the paper.

II. EXTENDED SELF SIMILARITY

A. Definition and Properties

The ESS process is a zero-mean Gaussian process $B_f(t)$ that satisfies

$$B_f(0) = 0, \quad (1)$$

and the following extended self-similar property:

$$\begin{aligned} \text{VAR}(B_f(s+p) - B_f(s)) &= f(p)\text{VAR}(B_f(t+1) - B_f(t)) \\ &= f(p)\sigma^2. \end{aligned} \quad (2)$$

Note that when $f(p)$ follows a hyperbolic law, i.e., $f(p) = |p|^{2H}$ where $0 < H < 1$, (2) reduces to the original self-similarity condition that defines an fBm process. The function $f(p)$ is known as the *structure function*. Many of the properties of random processes with stationary increments and structure functions are well presented in [16]. The structure function reflects the growth of the variance of increments of a process as the incremental length (or scale) increases. (In this correspondence, the incremental length Δx is related to the scale m by $\Delta x = C2^m$, where $m = 0, 1, 2, \dots$ and C can be any positive real number. This notion of scale is consistent with the notion of scale in wavelet analysis.)

We can use (1) and (2) to determine the correlation of the process $B_f(t)$ as

$$r_{B_f}(s, t) = \frac{\sigma^2}{2}[f(s) + f(t) - f(s-t)], \quad s, t \in \mathbf{R}. \quad (3)$$

The increments of the ESS process, i.e. $X_f(k; \Delta x) = B_f(\Delta x(k+1)) - B_f(\Delta xk)$, are stationary and have the correlation function

$$r_{X_f}(k; \Delta x) = \frac{\sigma^2}{2}[f(\Delta x(k+1)) + f(\Delta x(k-1)) - 2f(\Delta xk)], \quad k \in \mathbf{Z}. \quad (4)$$

When the structure function is hyperbolic, (4) gives the correlation function for dfGn. A nontrivial structure function and the corresponding parameterized version of (4) will be given as an example in Section III-A.

Many of the necessary and sufficient properties of the structure function are discussed in [8] and [16]. It should also be pointed out that the term "extended self-similarity" has been used in the area of turbulence physics to describe the hyperbolic relation between two different moments of the velocity increments for a given increment length [1]. Our use of extended self-similarity as expressed in (2) describes a totally different situation.

B. Discrete Haar Transform

The "whitening" effect of the wavelet transform for many ESS processes allows for a fast parameter estimation algorithm. In this section, we consider the application of the Haar transform on the increments of ESS processes. We concentrate on the Haar transform because the extended self-similarity condition (2) actually describes the behavior of the variance of the approximation coefficients, and there exists a simple closed form that describes the relationship between the variance of the detail wavelet coefficients and the structure function when the discrete Haar transform is applied. In contrast, the variance progression for discrete wavelets of higher regularity can only be expressed as a complicated cascade of the convolutional product of the structure function and the wavelet filters.

The discrete Haar transform provides a multiresolution decomposition of a discrete data sequence. Given the data sequence $a_0(k)$ (i.e., the finest scale approximation to the continuous signal), the higher scale approximation coefficients $a_m(k)$ and detail wavelet coefficients $d_m(k)$ of the Haar transform are computed recursively by

$$a_{m+1}(k) = \frac{1}{\sqrt{2}}(a_m(2k) + a_m(2k+1)), \quad (5)$$

$$d_{m+1}(k) = \frac{1}{\sqrt{2}}(a_m(2k) - a_m(2k+1)). \quad (6)$$

When the increments of an ESS process are put through the discrete Haar transform, the extended self-similarity property provides simple expressions of the correlation of the approximation and detail wavelet coefficients using the structure function as stated in the following theorem.

Theorem 1: Let $B_f(k)$ be a realization of an ESS process with incremental length Δx and $a_0(k)$ be the finest scale approximation of the increments of $B_f(k)$. Define the stochastic processes $a_m(k)$ and $d_m(k)$ to be the approximation and detail wavelet coefficients, respectively, of the Haar transform as given in (5) and (6). Then, the following hold:

- a) For fixed scale m , the correlation of $a_m(k)$ is

$$r_{a_m}(k) = 2^{-m} r_{X_f}(k; 2^m \Delta x) \quad (7)$$

where $r_{X_f}(k)$ is given in (4).

- b) For fixed scale m , $d_m(k)$ is stationary, and the variance of $d_m(k)$ is

$$\sigma_m^2 = r_{d_m}(0) = \sigma^2 2^{-m} (4f(2^{m-1} \Delta x) - f(2^m \Delta x)). \quad (8)$$

Proof: Since $a_0(k) = X_f(k; \Delta x)$, it is easy to see through (5) that

$$a_m(k) = 2^{-m/2} \sum_{i=0}^{2^m-1} X_f(2^m k + i; \Delta x) = 2^{-m/2} X_f(k; 2^m \Delta x)$$

and (7) follows. The stationarity of $d_m(k)$ is due to the fact that the process is derived by passing the stationary process $a_{m-1}(k)$ through a linear filter. Then, (6) and (7) implies

$$r_{d_m}(k) = 2^{-m} (2r_{X_f}(2k; 2^{m-1} \Delta x) - r_{X_f}(2k+1; 2^{m-1} \Delta x) - r_{X_f}(2k-1; 2^{m-1} \Delta x)).$$

By setting $k=0$ and using (4), (8) follows. \square

Although the Haar transform is not regular enough to effectively decorrelate fBm processes with $H \in (1/2, 1)$ [3], it was shown in [7] that the Haar transform can "whiten" fBm increments for all $H \in (0, 1)$. It turns out that the Haar transform can also effectively decorrelate ESS increments, that is, a technique originated in [12] and used by Tewfik and Kim in [14] can verify that the detail wavelet coefficients of the Haar transform have a correlation structure that decays faster than the original ESS increments as long

as the correlation of the stationary ESS increments decay over time. Specifically, when the correlation structure of (4) is treated as a continuous function, the function will be continuously differentiable if the structure function is continuously differentiable. Based on [14], it can be argued that if a wavelet filter of regularity R is used for discrete wavelet transform (DWT) implementation ($R=1$ for the Haar transform), the correlation of detail wavelet coefficients is bounded by

$$E[d_m[k]d_n[l]] \leq \sup_{0 \leq k', l' < 2R} \left| \frac{d^{2R} r[t]}{dt^{2R}} \right|_{t=2^m k - 2^{n-1} - k' + l'}. \quad (9)$$

If the structure function leads to increments that have some terms decaying exponentially and other terms decaying hyperbolically (e.g., fBm), the correlation of detail wavelet coefficients decays faster than that of original ESS increments because of (9). The faster decay for the exponential terms is due to the larger sampling period at higher scales, whereas the faster convergence of the hyperbolic terms was verified in [7]. The "whitening" effect of the Haar transform on increments of ESS processes will be verified in Section III-A. Although there is decay in correlation of wavelet coefficients as the time domain overlap decreases, there is, however, significant correlation between coefficients of different scales with overlapping temporal support. As a result, the correlation structure of the stationary wavelet coefficients is usually banded. Examples of the banded structure will also be presented in Section III-A.

C. Discrete Processes

When processing signals with the computer, a finite discrete set of data samples is all that can be considered. Thus, we have to use discrete correlation models. The ESS model provides a continuous model that can be sampled at intervals of Δx so that one only needs to know the correlation at integer multiples of Δx . By considering sampled ESS processes, the increments with incremental length Δx are the finest resolution increments available and serve as the stationary building block of the sampled ESS process. For convenience, we will set $\Delta x = 1$ when discussing sampled ESS processes. It is easy to show that any stationary discrete process can constitute the increments of a discrete ESS process because summing the stationary processes $X(k)$, i.e., $B(k) = \sum_{i=0}^{k-1} X(i)$, will create a nonstationary process with a well-defined correlation function.

III. ASYMPTOTIC FBM

A. Definition

The goal is to find a model whose correlation decays asymptotically like a fractal but where the short-term correlations differ from the normal dfGn model. (It is worthwhile to comment that dfGn for $0 < H < 1/2$ is a different process than dfGn for $1/2 < H < 1$ and that we find it difficult to expand the dfGn for the two processes into the same extended model.) We propose the following structure function

$$f(s) = \frac{A-1}{1-|\rho|} (|\rho|^{|s|} - 1) + A|s|^{2H} \quad (10)$$

where

$$A = \frac{2H + \rho(2-2H)}{2H - \rho(2-2H)}, \quad 1/2 < H < 1, \quad -1 < \rho < G(H). \quad (11)$$

It is shown in [8] that this structure function is well defined. A plot of $G(H)$ is given in Fig. 1. Note that (10) does not provide a valid continuous ESS process because as s goes to zero, $f(s)$ violates the positivity condition for variance.

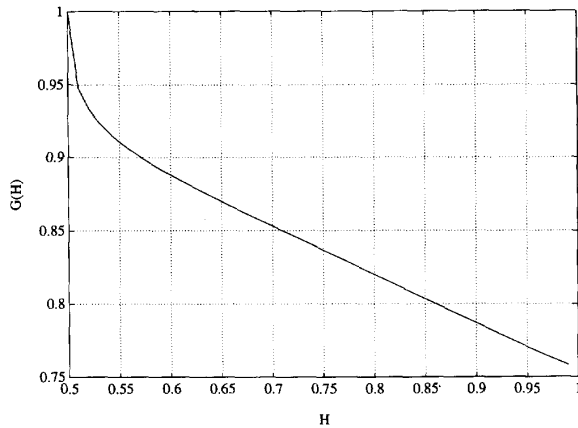


Fig. 1. Maximum possible value of ρ for a given value of H in the afBm model.

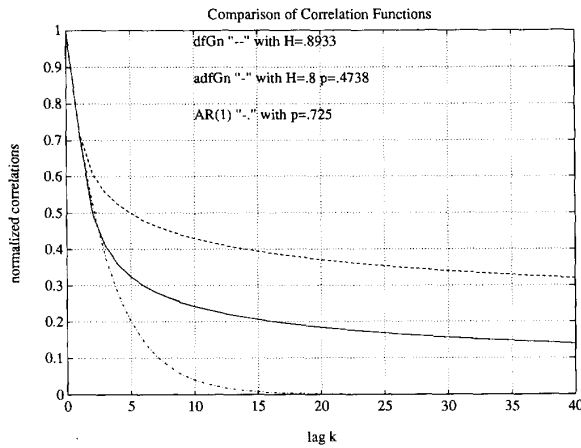


Fig. 2. Comparison of the correlation for three different adfGn models with the same variance and same correlation at lag one.

The resulting correlation function of the finest scale increments by (4) is

$$r_f(k) = \begin{cases} \sigma^2, & k = 0, \\ \frac{\sigma^2}{2} [(A-1)(1-|\rho|)|\rho|^{k-1} + A(|k+1|^{2H} + |k-1|^{2H} - 2|k|^{2H})], & k = 1, 2, \dots \end{cases} \quad (12)$$

The corresponding ESS increment model is called the *asymptotic dfGn* (adfGn). The shape of the adfGn model is controlled by two parameters where ρ provides a transient correlation effect, whereas H introduces the long-term fractal structure. The coefficient A is chosen so that when $\rho = 0$, the model is simply dfGn, and when $H = 1/2$, the structure function provides AR(1) increments. Moreover, the corresponding nonstationary discrete ESS model behaves asymptotically as fBm for coarse scales and will be referred to as asymptotic fBm (afBm). The parameter ρ will smooth out the finer scales, and the parameter H controls the roughness of the process at coarser scales. Fig. 2 demonstrates how adfGn expands on AR(1) and dfGn models by showing the correlation function for various values of ρ and H when the $\sigma^2 = 1$ and the correlations at lag one are equal. Plots of afBm at scales $m = 4$ and $m = 0$ are shown in Fig. 3 with $\rho = 0.85$ and $H = 0.65$. Note that the realization at different scales is scaled in a similar way as in [13] according to the H parameter, which

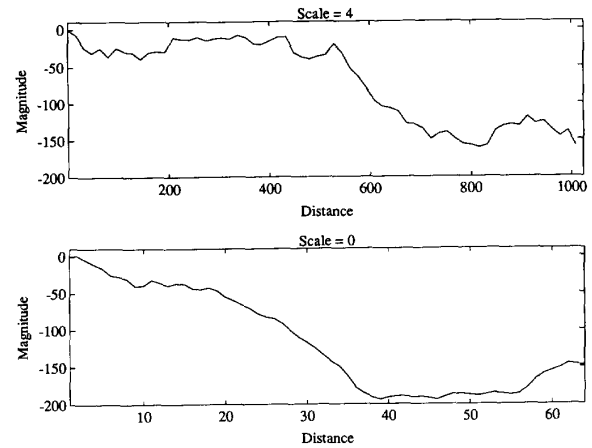


Fig. 3. Realization of afBm with $\rho = 0.85$ and $H = 0.65$ at scales $m = 4$ (top) and $m = 0$ (bottom).

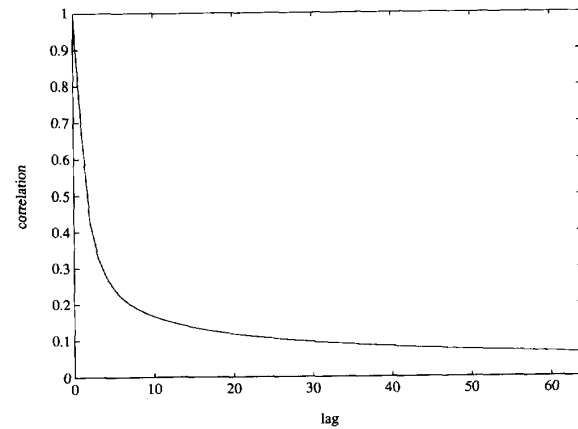


Fig. 4. Correlation decay of an adfGn process with $\rho = 0.5$ and $H = 0.75$.

represents the asymptotic fractal structure. It is evident that the afBm realization is smoother at finer scales, whereas at coarser scales, the process is as rough as the fBm with the same value of H .

The correlation decay of adfGn is evident in (12). The "whitening" effect of the Haar transform on an adfGn process is shown in Figs. 4-6. The figures also demonstrate the banded structure of the detail wavelet correlation matrix.

B. Parameter Estimation

The decorrelation of adfGn by the discrete Haar transform and the algorithms for fBm estimation presented in [7] and [15] motivates a simple parameter estimation algorithm that provides estimates of parameters ρ , H , and σ^2 of the adfGn model. Suppose that given the input data M scales of the Haar transform can be computed, and for each scale m , there are $N(m)$ Haar detail coefficients. Since the input data is assumed Gaussian (ESS processes are Gaussian by definition), the Haar coefficients are Gaussian. Then, using the assumption that the coefficients are uncorrelated, a log likelihood function based on the distribution of the wavelet coefficients is simply

$$L(\rho, H, \sigma^2) = -\frac{1}{2} \sum_{m=1}^M N(m) \left[\frac{\hat{\sigma}_m^2}{\sigma_m^2} + \log(2\pi\sigma_m^2) \right] \quad (13)$$

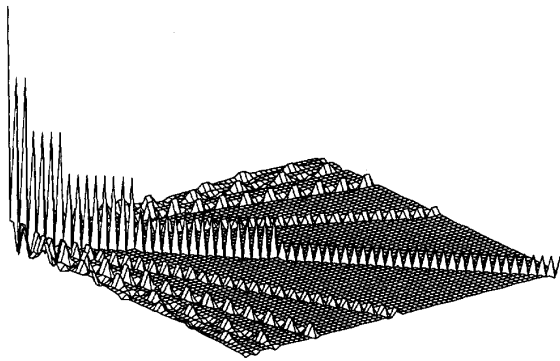


Fig. 5. Theoretical correlation matrix of the Haar wavelet coefficients of an adfGn process with $\rho = 0.5$ and $H = 0.75$.

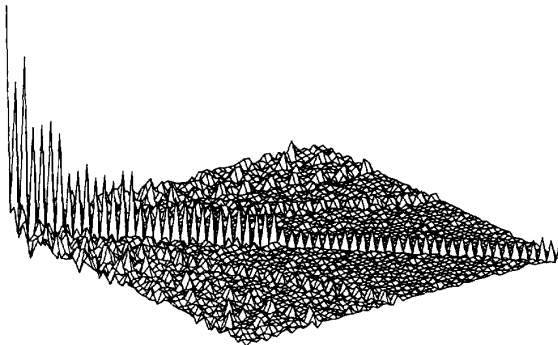


Fig. 6. Experimental correlation matrix of the Haar wavelet coefficients of an adfGn process with $\rho = 0.5$ and $H = 0.75$.

where $\hat{\sigma}_m^2$ is the sampled variance of the Haar coefficients at scale m , and σ_m^2 is provided by (8) for the adfGn structure function. Since the value of σ^2 that maximizes (13) for fixed ρ and H is

$$\sigma^2 = \frac{\sum_{m=1}^M N(m) \hat{\sigma}_m^2 / \bar{\sigma}_m^2}{\sum_{m=1}^M N(m)} \quad (14)$$

where $\bar{\sigma}_m^2$ is evaluated from (8) for $\sigma^2 = 1$, then (13) can be reexpressed as a function of ρ and H . The parameter estimation algorithm is as follows. First, compute the Haar transform coefficients from the data sample. Then, calculate the sample variance of the coefficients at each scale, and maximize (13) (where (14) is substituted inside) over ρ and H by a steepest descent type of algorithm to obtain the estimates $\hat{\rho}$ and \hat{H} . Finally, obtain $\hat{\sigma}^2$ through (14). The attractive feature of this algorithm is that it requires no matrix inversion. The estimation algorithm for filtered fractal presented in [2] is an estimate-maximize (EM) algorithm that requires the inversion of a $N \times N$ matrix for every estimate step where N is the data length, and it can take many estimate steps for the EM algorithm to converge. The ESS models appear to provide a method to generalize a fBm that provides faster algorithms than filtered fractals. However, since the filtered fractal and adfGn models are different, the accuracy of the estimated parameters cannot be directly compared.

C. Simulations

To test the estimation algorithm for the adfGn, we created 64 realizations of an adfGn of length 1024 samples with different parameters using the Cholesky decomposition technique [10] via the Levinson recursion [5], and we calculated estimates of H , ρ ,

TABLE I
MEANS AND STANDARD DEVIATIONS FOR THE ESTIMATES OF THE PARAMETERS OF adfGn WHERE $\sigma^2 = 1$ AND $H = 1/2$, $\rho = 0$ ARE THE INITIAL ESTIMATES

True Parameters		ρ		H		σ^2	
H	ρ	mean	std	mean	std	mean	std
.9	.5	.5187	.1539	.8809	.0749	1.1920	.8527
.9	0	-.0076	.2028	.8901	.0476	1.1205	.5711
.9	-.5	-.3458	.2435	.8756	.0377	0.9597	.2007
.7	.5	.4911	.0949	.6920	.0633	1.0142	.0772
.7	0	-.0283	.1578	.7020	.0477	1.0031	.0612
.7	-.5	-.2151	.2044	.6434	.0525	1.0007	.0454
.5	.5	.4419	.0585	.5465	.0828	1.0049	.0621
.5	0	-.0253	.1198	.5049	.0582	0.9978	.0379
.5	-.5	-.0479	.1632	.3452	.0885	0.9953	.0412

TABLE II
MEANS AND STANDARD DEVIATIONS FOR THE ESTIMATES OF THE PARAMETERS OF adfGn WHERE $\sigma^2 = 1$ AND TRUE PARAMETERS ARE THE INITIAL ESTIMATES

True Parameters		ρ		H		σ^2	
H	ρ	mean	std	mean	std	mean	std
.9	.5	.5186	.1403	.8839	.0575	1.1649	.8388
.9	0	-.0102	.1999	.8912	.0460	1.1232	.5704
.9	-.5	-.4056	.2417	.8824	.0379	0.9829	.2003
.7	.5	.5004	.0896	.6841	.0657	1.0094	.0780
.7	0	-.0287	.1583	.7021	.0479	1.0032	.0611
.7	-.5	-.4871	.1412	.6948	.0267	1.0070	.0464
.5	.5	.4813	.0374	.4929	.0494	1.0002	.0605
.5	0	-.0253	.1198	.5049	.0582	0.9978	.0379
.5	-.5	-.4627	.1688	.4795	.0540	0.9959	.0418

and σ^2 . Table I shows the results with initial estimates $H = 1/2$ and $\rho = 0$ (white noise), and Table II shows the results when the initial estimates are the parameter values used to generate the test data. We see from Tables II and III that the descent algorithm finds equally good estimates with the two different initial conditions for most cases. However, the steepest descent algorithm could find the wrong local minimum with certain initial estimates in some cases. Obviously, further study is necessary to find a smart way to circumvent the problem that the likelihood function is not convex. It is also interesting to note that the algorithm can find a better estimate for H than ρ . One reason for this phenomena is that the fractal structure is consistent for all scales, whereas the exponential structure dies out into the Brownian structure at coarser scales. In other words, the fractal structure carries more information at the larger scales. Overall, the performance of the proposed parameter estimation algorithm is promising.

IV. CONCLUSIONS

The idea of extending the concept of self-similarity presents a much richer class of nonstationary process with stationary increments than fBm. The structure function concept provides new tools for signal and image modeling. Since every discrete ESS process can be represented at the finest available scale by a stationary process with an otherwise arbitrary correlation function, one can use the structure function to create nonstationary (the ESS process) or stationary (the ESS increment) models. In this correspondence, one possible structure function using two parameters, i.e., ρ and H , was introduced to show how short-term correlations can be added to the fBm model.

The whitening property of the discrete Haar transform is useful for creating a fast parameter estimation algorithm for the new model.

ACKNOWLEDGMENT

The authors wish to thank the anonymous reviewer who informed us about the theory of random processes with stationary increments and pointed out the use of the "extended self-similarity" term in the area of turbulence physics.

REFERENCES

- [1] R. Benzi *et al.*, "Extended self-similarity in turbulent flows," *Phys. Rev. E*, vol. 48, pp. R30-R32, July 1993.
- [2] M. Deriche and A. H. Tewfik, "Signal modeling with filtered discrete fractional noise processes," *IEEE Trans. Signal Processing*, vol. 41, pp. 2839-2849, Sept. 1993.
- [3] P. Flandrin, "Wavelet analysis and synthesis of fractional Brownian motion," *IEEE Trans. Inform. Theory*, vol. 38, pp. 910-917, Mar. 1992.
- [4] C. W. Granger and R. Joyeux, "An introduction to long memory time series models and fractal differencing," *J. Time Series Analysis*, vol. 1, no. 1, 1980.
- [5] S. Haykin, *Adaptive Filter Theory*. Englewood Cliffs, NJ: Prentice Hall, Inc., 1991.
- [6] J. R. M. Hosking, "Fractional differencing," *Biometrika*, vol. 68, no. 1, pp. 165-176, 1981.
- [7] L. M. Kaplan and C.-C. J. Kuo, "Fractal estimation from noisy data via discrete fractional Gaussian noise (dfGn) and the Haar basis," *IEEE Trans. Signal Processing*, vol. 41, pp. 3554-3562, Dec. 1993.
- [8] —, "Signal modeling with extended self-similar processes," Tech. Rep. SIPI 242, Univ. of Southern Calif., Sept. 1993.
- [9] M. S. Keshner, "1/f noise," *Proc. IEEE*, vol. 70, pp. 212-218, Mar. 1982.
- [10] T. Lundahl, W. J. Ohley, S. M. Kay, and R. Siffert, "Fractional Brownian motion: A maximum likelihood estimator and its application to image texture," *IEEE Trans. Med. Imaging*, vol. 5, pp. 152-161, Sept. 1986.
- [11] B. B. Mandelbrot and J. W. V. Ness, "Fractional Brownian motions, fractional noises and applications," *SIAM Rev.*, vol. 10, pp. 422-437, Oct. 1968.
- [12] Y. Meyer, *Ondelettes et Operateurs*. Paris: Herman, 1990.
- [13] H. O. Peitgen and D. Saupe, Eds., *The Science of Fractal Images*. New York: Springer-Verlag, 1988.
- [14] A. H. Tewfik and M. Kim, "Fast positive definite linear system solvers," *IEEE Trans. Signal Processing*, vol. 42, pp. 572-585, Mar. 1994.
- [15] G. W. Wornell and A. V. Oppenheim, "Estimation of fractal signals from noisy measurements using wavelets," *IEEE Trans. Signal Processing*, vol. 40, pp. 611-623, Mar. 1992.
- [16] A. M. Yaglom, *Correlation Theory of Stationary and Related Random Functions*. New York: Springer-Verlag, 1987.

A Simple Scheme for Adapting Time-Frequency Representations

Douglas L. Jones and Richard G. Baraniuk

Abstract—We propose a simple, efficient technique for continuously adapting time-frequency and time-scale representations over time. The procedure computes a short-time quality measure of the representation for a range of values of a free parameter and estimates the optimal parameter value maximizing the quality measure via interpolation.

I. INTRODUCTION

Most time-frequency representations (TFR's) employ some kind of smoothing kernel, window, or filter to reduce noise and cross-components [1], [2]. The choice of kernel dramatically affects the appearance and quality of the resulting TFR. It has been shown that, according to several different measures of performance, the optimal kernel depends on the signal being analyzed [3]–[5]. Therefore, utilization of any fixed kernel severely limits the class of signals for which the resulting time-frequency representation can perform well.

As an example, consider the signal shown in Fig. 1. It contains several narrow pulses, two sinusoids that overlap in time, and a Gaussian component. Fig. 2 illustrates three short-time Fourier transforms (STFT's) of this signal computed using Gaussian windows of varying lengths. A short window (Fig. 2(a)) matches the pulse components well but smears the sinusoidal and Gaussian components in the frequency direction. A medium-length window (Fig. 2(b)) matches the Gaussian component well but smears the pulse and sinusoidal components in both the time and frequency directions. A long window (Fig. 2(c)) matches the sinusoidal components but smears the pulse and Gaussian components in the time direction. These figures illustrate the fundamental drawback of the STFT: It is impossible to obtain simultaneously good time and good frequency resolution using a single fixed window. The continuous wavelet transform [6] suffers from the same tradeoff, although in this case the tradeoff is a function of frequency. Moreover, a related tradeoff between time-frequency resolution and cross-term suppression applies to the kernel function in all bilinear (Cohen's class) time-frequency representations. In short, no TFR employing a fixed window, wavelet, or kernel performs well for all signals.

Due to this fundamental limitation of fixed windows or kernels, several researchers have developed signal-dependent or adaptive TFR's (see [3]–[5], [7]–[9] and the references in [4]). These methods often exhibit performance far surpassing that of fixed-kernel representations; however, they are either very computationally expensive or perform only off-line, block analysis of short signals. Thus, a need exists for simple, time-adaptive, computationally efficient TFR's suitable for real-time, on-line applications.

This paper presents a new scheme for adapting a TFR with a single free parameter. Section II describes the optimization formulation,

Manuscript received August 20, 1992; revised May 16, 1994. This work was supported by: the National Science Foundation, Grant No. MIP 90-12747; the Joint Services Electronics Program, Grant No. N00014-90-J-1270; and the Sound Group of the Computer-based Education Research Laboratory at the University of Illinois. The associate editor coordinating the review of this paper and approving it for publication was Prof. Mysore Raghuvver.

D. L. Jones is with the Coordinated Science Laboratory, University of Illinois, Urbana, IL 61801 USA.

R. G. Baraniuk is with the Department of Electrical and Computer Engineering, Rice University, Houston, TX 77251-1892 USA.

IEEE Log Number 9406013.